

RSC Medicinal Chemistry

Accepted Manuscript

This article can be cited before page numbers have been issued, to do this please use: Q. Yu, Z. Liu, J. Liu and L. Bai, *RSC Med. Chem.*, 2026, DOI: 10.1039/D6MD00223D.



This is an Accepted Manuscript, which has been through the Royal Society of Chemistry peer review process and has been accepted for publication.

Accepted Manuscripts are published online shortly after acceptance, before technical editing, formatting and proof reading. Using this free service, authors can make their results available to the community, in citable form, before we publish the edited article. We will replace this Accepted Manuscript with the edited and formatted Advance Article as soon as it is available.

You can find more information about Accepted Manuscripts in the [Information for Authors](#).

Please note that technical editing may introduce minor changes to the text and/or graphics, which may alter content. The journal's standard [Terms & Conditions](#) and the [Ethical guidelines](#) still apply. In no event shall the Royal Society of Chemistry be held responsible for any errors or omissions in this Accepted Manuscript or any consequences arising from the use of any information it contains.

ARTICLE

Recent advances of piperine and its derivatives as potential anticancer agents

Qi-Hua Yu,^a Zhiyan Liu,^a Jiazheng Liu^a and Li-Ping Bai^{*abc}Received 00th January 20xx,
Accepted 00th January 20xx

DOI: 10.1039/x0xx00000x

Piperine, a crucial ingredient of the plant *Piper nigrum*, exhibits a broad spectrum of biological activities and has attracted interest as a potential anticancer agent. With a low yield in natural resources, chemists have developed several synthetic methods for piperine. In addition, low water solubility and poor bioavailability of piperine have significantly limited its therapeutic application. Structural modification, particularly at its piperidine moiety, enables the introduction of diverse functional groups to afford piperine derivatives with improved anticancer potency and favorable pharmacodynamic profiles. This article reviews the recent advances (from 2012 to 2025) in the structural characterization, chemical synthesis, biosynthesis, anticancer profile, structural modification, and structure activity relationship of piperine, which may provide useful direction for the development of more effective piperine-based anticancer candidates or agents.

Keywords: Piperine; Synthesis; Anticancer activity; Structural modification; Structure activity relationship

1. Introduction

Nowadays, cancer is a significant public health problem in the 21st century, accounting for almost one in six deaths (16.8%).¹ There are several approaches on the current cancer treatment, such as chemotherapy, surgery, radiotherapy and biotherapy. Chemotherapy, as a conventional cancer therapy, still faces enormous challenges owing to drug resistance, toxicity, and target mutations.² The number of patients demanding chemotherapy is expected to increase by 53% annually from 9.8 million in 2018 to 15.0 million in 2040.³ Thus, it is urgent to discover novel anticancer drugs with higher efficacy and lower toxicity for a growing demand of chemotherapy drugs. Natural products have long been a valuable resource for drug discovery due to their chemical diversity and abundant biological activity while relatively low toxicity property.⁴

Piperine (Fig. 1), as a natural alkaloid, is originally isolated from *Piper nigrum* by Danish scientist Hans Christian Orsted in 1819.⁵ Piperine is a weak base in nature, which upon alkaline hydrolysis decomposes to piperidine and piperic acid derivative.⁶ The structure of piperine (Fig. 1) is composed of three parts: (1) Aromatic region (1,3-benzodioxole group), (2) Aliphatic chain region (butadiene chain), and (3) Amide region (a piperidine ring connected with α , β -unsaturated carbonyl moiety).⁷ In addition, piperine contains four cis-trans isomeric

structures (Fig. 2) named as the *trans-trans* isomer (piperine), *cis-cis* isomer (chavicine), *cis-trans* isomer (isopiperine), and *trans-cis* isomer (isochavicine).⁸

Piperine is distributed in several members of *Piperaceae* family, such as *Piper nigrum*,⁹ *P. chaba*,¹⁰ *P. longum*,¹¹ and *P. guineense*¹² as the main secondary metabolites. Additionally, piperine has attracted considerable attention from pharmaceutical chemist and nutritional expert attention due to its multiple biological activities, including anti-cancer,¹³ anti-oxidant,¹⁴ anti-inflammatory,¹⁵ neuroprotection,¹⁶ hepatoprotection,¹⁷ antidepressant,¹⁸ and anti-diabetes¹⁹ effects. Hence, there is a strong demand for piperine for further research and development. Despite several biological properties of piperine, its low solubility in water and limited bioavailability have constrained its clinical application, as high doses administration of piperine may be required and can be associated with toxicity.²⁰ Moreover, the low concentration of piperine in *Piper nigrum* and its low extraction yield have also limited the practical application and industrial development of piperine.²¹ To overcome these limitations, scientists have not only developed several synthetic methods to obtain piperine but also synthesized piperine derivatives to enhance their efficacy.²²

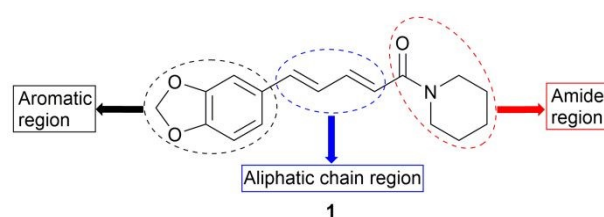


Fig. 1 The structure of piperine.

With an aim to provide deeper insights into anticancer development of piperine derivatives and expand their

^a State Key Laboratory of Mechanism and Quality of Chinese Medicine, Macau Institute for Applied Research in Medicine and Health, Macau University of Science and Technology, Taipa, Macau 999078, China.

^b Guangdong-Macao Joint Laboratory for Innovative Drug Research on TCM and Natural-Derived Small RNAs, Macau University of Science and Technology, Taipa, Macau 999078, China.

^c Zhuhai M.U.S.T. Science and Technology Research Institute, Hengqin New District, Zhuhai, Guangdong, 519031, China E-mail: lpbai@must.edu.mo



therapeutic potential, this review summarizes recent advances (from 2012 to 2025) in piperine research, including structural characterization, chemical synthesis, biosynthesis, anticancer activity, structural modifications, and structure activity relationship (SAR) studies.

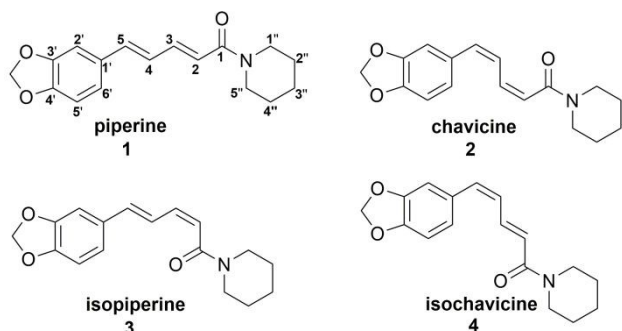


Fig. 2 The isomers of piperine.

2. Structural characterization of piperine

Piperine is typically found in the yield range of 1.7-7.4% from the raw black pepper materials.⁹ In addition, the main pungency of pepper is caused by piperine. Although the other three isomers are only slightly pungent and are found in very low concentration in pepper, piperine is gradually converted into chavicine on storage, leading to loss of pungency.²³ Therefore, several technical methods are needed to determine the chemical structures of piperine and its isomers. In the past few decades, the spectroscopic techniques, including ultraviolet spectroscopy (UV), nuclear magnetic resonance (NMR), mass spectrometry (MS), and infrared spectroscopy (IR) have been widely used to elucidate the structural characterization of piperine.

Table 1 Comparison of the structural characterization data of piperine and its isomers.

Compound	1	2	3	4
UV λ_{max} (nm)	340	318	332	333
NMR $J_{2,3}$ (Hz)	14.7 (<i>trans</i>)	11.1 (<i>cis</i>)	11.2 (<i>cis</i>)	14.7 (<i>trans</i>)
NMR $J_{3,4}$ (Hz)	8.5	11.0	11.2	11.8
NMR $J_{4,5}$ (Hz)	15.0 (<i>trans</i>)	11.1 (<i>cis</i>)	15.6 (<i>trans</i>)	11.8 (<i>cis</i>)

Due to the geometric isomerism in the two double bonds, piperine **1** (Table 1) is estimated by UV spectroscopy via the UV maximum absorption wavelength at 340 nm, while chavicine **2**, isopiperine **3**, and isochavicine **4** are at 318, 332, 333 nm respectively.²⁴ Furthermore, as shown in Table 1, the difference between piperine and its isomers in the coupling constants for the olefinic protons (*cis*- $J_{(H,H)} \approx 11$ Hz, *trans*- $J_{(H,H)} \approx 15$ Hz) makes it possible to determine the configuration of the isomers in ¹H spectrum.²⁴ The mass spectrum of piperine²⁵ is characterized by the fragment ions (*m/z*): 285 molecular ion (*M*⁺), 201 from cleavage at the C-N bond, and 173 representing loss of -CO (28) from *m/z* 201, followed by loss of -CH₂O (30) and -CO (28) to form *m/z* 143 and 115, respectively. The genesis of these fragment ions²⁵⁻²⁷ can be rationalized, as shown in Fig. 3. In addition, the IR spectrum²⁴ of piperine exhibits a carbonyl stretching band in the α , β -unsaturated amide moiety, which

appears at approximately 1650 cm⁻¹. The presence of alkene C-H, aromatic C-H and aliphatic C-H stretching bands appear at approximately 3080 cm⁻¹, 3030 cm⁻¹, and 2910 cm⁻¹, respectively. The stretch of the C=C of aromatic rings in the range of 1606-1483 cm⁻¹ are observed, while stretching of the alkenes C=C are observed at approximately 1620 cm⁻¹. The asymmetric and symmetrical stretching of the methylenedioxy group varies between 1257-1226 and 1143-1128 cm⁻¹, respectively.²⁶

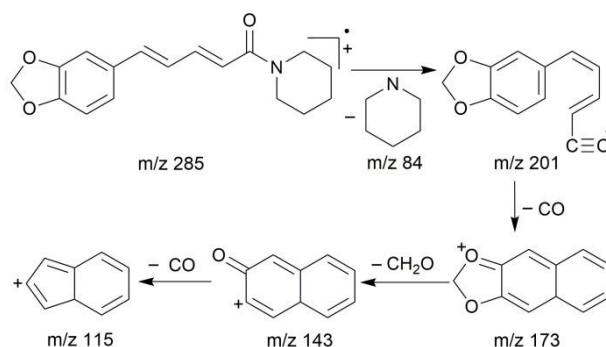


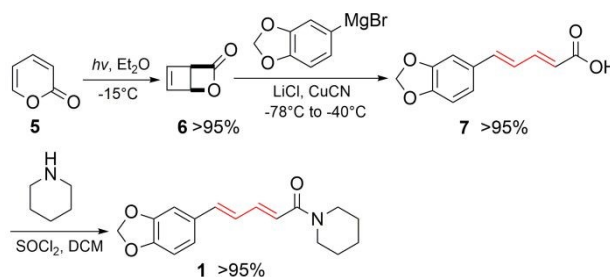
Fig. 3 Mass spectral fragmentation pattern of piperine.

Overall, these spectroscopic data (UV, NMR, MS, and IR) collectively support the structural assignment of piperine and facilitate identification of piperine-type amides in future studies.

3. Chemical synthesis of piperine

Although piperine is traditionally extracted from black pepper,²¹ the extraction supply still may be constrained by multistep procedure and variable efficiency. To address these issues, scientists have continued to develop several synthetic strategies for the artificial synthesis of piperine. In this section, we summarize the recent synthetic strategies for piperine.

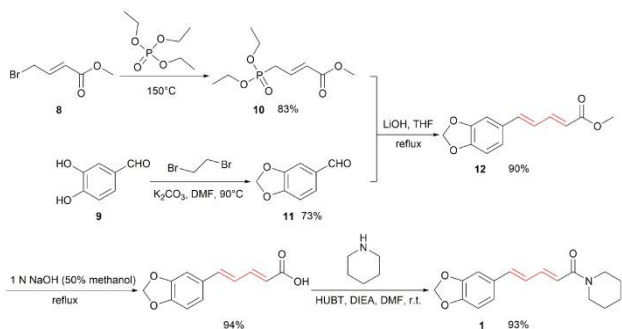
In 2019, Bauer and co-workers²⁸ reported the quantitative and stereoselective synthesis of piperine (Scheme 1) by using 2-pyrone (**5**) as the starting compound. The bicyclo [2.2.0] lactone (**6**) was prepared from 2-pyrone (**5**) via photochemical synthesis. Subsequently, lactone (**6**) was reacted with copper cyanide (CuCN), lithium chloride (LiCl) and Grignard reagent of the piperonal to obtain the *E*, *E*-diene isomer (**7**) in the copper-mediated nucleophilic addition and electrolytic ring opening reaction. At last, the isomer (**7**) was converted into acyl chloride and then reacted with piperidine to afford piperine (**1**) in more than 95% yield.



Scheme 1 Bauer et al. method for synthesis of piperine.

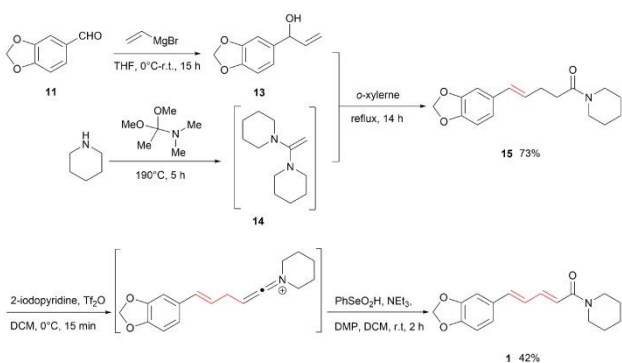


Tian et al.²⁹ developed an alternative route by using methyl (E)-4-bromobut-2-enoate (**8**) and 3,4-dihydroxybenzaldehyde (**9**) as starting materials, (Scheme 2) and obtained intermediate **10** and **11** respectively via nucleophilic substitution reactions. Later, the procedure involved a vinylogous modified Wittig condensation between piperonal (**10**) and the prepared phosphorus ylide reagent (**11**) under LiOH as a base in THF to give methyl piperate (**12**). This transformation is a traditional method to achieve stereoselective control over the double bond configurations.²⁹⁻³¹ Then, piperine (**1**) was prepared by the hydrolysis of **12** and subsequent amidation with piperidine in an overall yield of 65%.



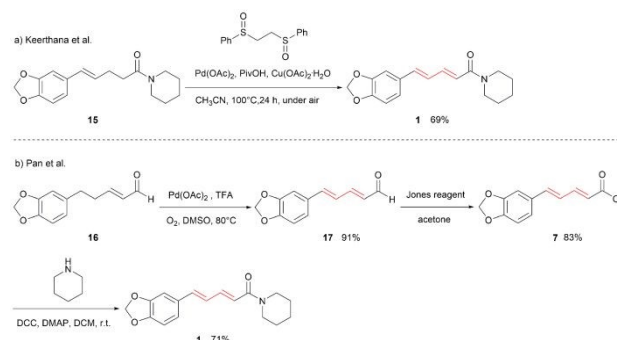
Scheme 2 Tian et al. method for synthesis of piperine.

Teskey and co-workers³² reported a method (Scheme 3) for the selective α,β -dehydrogenation of amides, depending on electrophilic activation coupled to in situ selective selenium-mediated dehydrogenation. They published an alternative three-step synthesis starting from the commercially available aldehyde (**11**). After the transformation of **11** into the allylic alcohol (**13**), this compound was treated with the prepared 1,1-diamino alkene (**14**) in refluxing xylene to yield the γ,δ -unsaturated amide (**15**) by a modified Claisen–Eschenmoser rearrangement. Further, compound **15** was reacted with Tf₂O and 2-iodopyridine via electrophilic amide activation, and the resulting mixture was subjected to a seleninic acid (PhSe(O)OH)-mediated selective substitution and elimination reaction in the presence of Dess–Martin periodinane (DMP) and Et₃N, affording a late-stage α,β -dehydrogenation tool to access the conjugated amide motif of piperine (**1**) in 42 % yield.



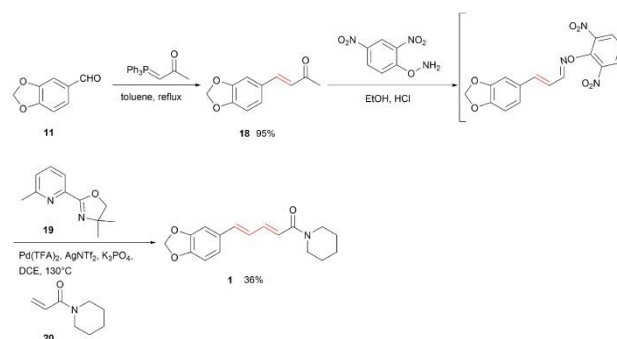
Scheme 3 Teskey et al. method for synthesis of piperine.

In 2022, Keerthana et al.³³ described the synthesis of piperine (Scheme 4a) via palladium-catalysed aerobic dehydrogenation of γ,δ -olefinic amides. In this method, γ,δ -unsaturated amide (**15**) was dehydrogenated in the presence of pivalic acid (PivOH), with Cu(OAc)₂·H₂O as cocatalyst, and 1,2-bis(phenylsulfinyl)ethane as ligand to obtain piperine (**1**) in a 69% yield. In addition, Pan group³⁴ also developed a new strategy (Scheme 4b) for the direct and efficient synthesis of piperine via forming (*E, E*)-dienone by a palladium-catalysed aerobic γ,δ -dehydrogenation of enone. Compound **16** was converted into *E, E*-dienal (**17**) in the presence of TFA under O₂, followed by oxidation with Jones reagent to acid and the condensation with piperidine to give piperine (**1**) in three steps with an overall yield of 54%.



Scheme 4 The palladium-catalysed aerobic dehydrogenation for piperine, (a) Keerthana et al. method and (b) Pan et al. method.

Li et al.³⁵ reported a β -carbon elimination strategy (Scheme 5) for alkene (sp²)-C(O) bonds to realize the olefination of unstrained enones via a vinyl palladium. Their strategy started from the conversion of aldehydes (**11**) to alkene intermediate (**18**) in the presence of phosphorus ylide reagent via the Wittig reaction. The compound **18** was then reacted with hydroxylamine reagent to afford 2,4-di-NO₂-phenyl-substituted oxime ether intermediate, which was subsequently subjected to oxidative addition of palladium, ligand (**19**)-promoted β -carbon elimination, further proceeded cross-coupling with alkene (**20**) to generate the piperine (**1**) in two step one pot reaction with 34% overall yield.



Scheme 5 Li et al. method for synthesis of piperine.

Since the earlier report of piperine synthesis by Tsuboi in 1979,³⁶ improvements and innovations have never stopped on geometric control of the diene and in operational simplicity

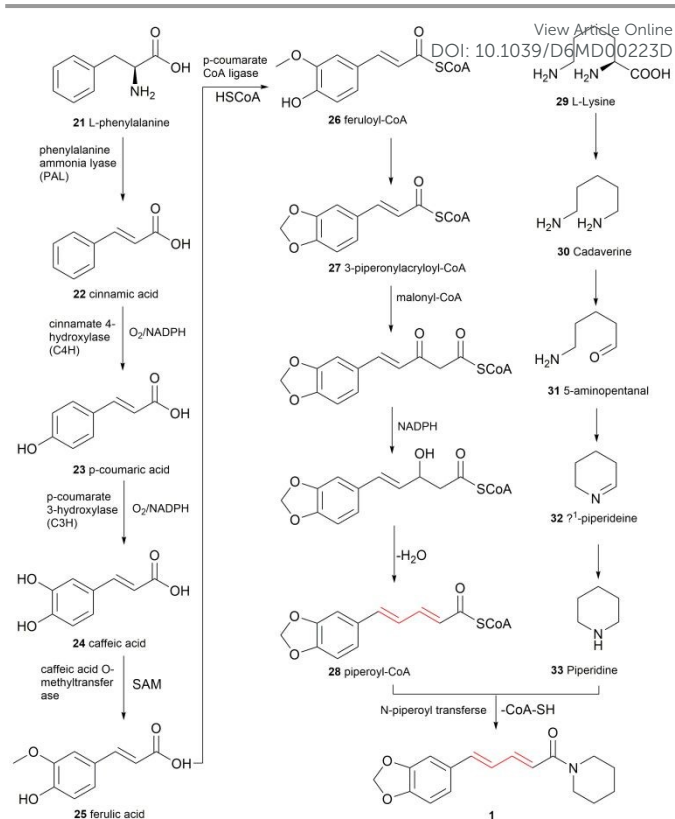


during its synthesis. Overall, recent advances in synthetic chemistry focus on two directions: (1) the efficient construction and stereocontrol of conjugated (*E,E*)-diene linkers; and (2) the development of catalytic dehydrogenation/activation strategies that facilitate the late-stage installation of α,β -unsaturated amides. From the synthesis perspective, piperic acid (or its activated acylating compound) serves as a practical intermediate for coupling with a diverse range of amine. Nevertheless, the main challenges persist in the stereocontrol of *E/Z* isomers.

4. Biosynthesis of piperine

The research³⁷ has shown that the complete biosynthetic process of piperine mainly consists of two key components, piperidine and piperoyl-coenzyme A. The piperidine heterocycle in piperine is derived from L-lysine, whereas the aromatic part of piperine is derived from L-phenylalanine via phenylpropanoid metabolism (Scheme 6).³⁸ In general, piperine, as an alkaloid of secondary metabolites, is biosynthesized through a series of reactions such as elimination, hydroxylation, condensation, decarboxylation, reduction, oxidative deamination and cyclization.^{39, 40}

In the biosynthetic pathway of the aromatic part in piperine^{38, 41} (Scheme 6), L-phenylalanine **21** as a precursor for a broad range of natural products is converted to cinnamic acid **22** by the enzyme phenylalanine ammonia lyase (PAL) via the elimination of ammonia. The derivatives of cinnamic acid **22**, such as *p*-coumaric acid **23** and caffeic acid **24**, are formed via hydroxylation catalysed by the enzyme in the presence of oxygen and reduced nicotinamide adenine dinucleotide phosphate (NADPH). Additionally, ferulic acid **25** is obtained from caffeic acid **24** via an enzyme-catalysed methylation reaction with the co-enzyme S-Adenosylmethionine (SAM). Thus, it is evident that cinnamic acid and its derivatives are the progenitors for phenylpropanoid compounds. Subsequently, feruloyl-CoA **26** is esterified by ferulic acid **25** and HSCoA with the *p*-coumarate CoA ligase, followed by the cyclization to obtain 3-piperonylacryloyl-CoA **27**. As depicted in Scheme 6, several studies^{37, 38} have proposed that 3-piperonylacryloyl-CoA **27** condenses with malonyl-CoA to form piperoyl-CoA **28**. Similar to the process of fatty acid biosynthesis, the extension on the chain of piperoyl-CoA **28** has been suggested via condensation with malonyl-CoA and intermediate **27** through the Claisen reaction, followed by selective reduction and dehydration reaction. However, the malonyl CoA-based chain elongation mechanism proposed for C-2 elongation remains hypothetical and requires direct enzymatic validation.^{40, 42}



Scheme 6 The hypothetical biosynthesis pathway for piperine.

Furthermore, in the biosynthetic pathway (Scheme 6) of the piperidine heterocycle,^{25, 43} L-lysine **29** is decarboxylated in the presence of the coenzyme pyridoxal phosphate (PLP) to afford cadaverine **30**. Subsequently, cadaverine **30** is subjected to oxidative deamination by the enzyme diamine oxidase to obtain an amino aldehyde **31**. The 5-aminopentanal **31** further undergoes cyclization to yield the imine, Δ^1 -piperideine **32**, followed by reduction with NADPH to generate piperidine **33**. Finally, piperine **1** is synthesized in plants from piperidine **33** and piperoyl-CoA **28**. Importantly, an acyltransferase from the shoots of *Piper nigrum* shoots³⁷ was reported to catalyse piperine formation from piperoyl-CoA and piperidine. This provides a viable biocatalytic strategy for future chemoenzymatic synthesis and late-stage acylation.

5. Anticancer profiles of piperine

Piperine has been reported to exert diverse anticancer effects through multiple mechanisms, including cancer cell cycle arrest and induction of apoptosis and autophagy. Piperine has also been reported to inhibit angiogenesis, invasion, and metastasis through modulating the activities of cancer-relevant enzymes and transcription factors.^{2, 44} Furthermore, piperine has been investigated as a chemosensitizer to reverse the multidrug resistance (MDR) in cancer cells through its multiple proposed mechanisms (Fig. 4).⁴⁵

5.1 Cell cycle arrest, apoptosis, and autophagy

Cancer is associated with irregular, excessive, and continuous proliferation of cells.⁴⁶ Several studies have demonstrated



piperine-induced cell cycle arrest, apoptosis and autophagy in various cancer cell lines and tumor models. Greenshields et al.⁴⁷ showed piperine decreased the expression of cell cycle G1 regulators (cyclin D3, CDK4, and E2F1) and G2 regulators (cyclin B, CDK1, Cdc25C), as well as increased expression of p21^{Waf1/Cip1} on the MDA-MB-468 cell line to reduce percentage of cells in the G2 phase. Chang et al.¹³ also reported that piperine decreased cyclin E expression and increased p27 levels, consistent with G1 cell cycle arrest in DLD-1 cell line. In addition, piperine suppressed the phosphoinositide 3-kinase (PI3K)/Akt signaling while increasing the p-extracellular signal-regulated kinase (ERK) levels, which was associated with enhanced apoptotic responses in DLD-1 cells. Besides, Greenshields group⁴⁷ reported piperine promoted the release of cytochrome c (cyt-c) and second mitochondria-derived activator of caspases/direct inhibitor of apoptosis (IAP)-binding protein with low propidium iodide (pi) (Smac/DIABLO) from the mitochondria to induce caspase-dependent apoptosis in the MDA-MB-468 cell line, without the functional p53. *In vivo*, intratumoral administration of piperine (0.2 mg/kg) inhibited the growth of MDA-MB-468 cell xenografts in female NOD/SCID nude mice. Han et al.⁴⁸ reported piperine downregulated anti-apoptotic protein (B-cell lymphoma-2 protein (Bcl-2)) and upregulated pro-apoptotic protein (Bcl-2-associated X protein (Bax)) and apoptotic marker (Cleaved Poly (ADP-ribose) polymerase (Cleaved PARP)) expression. Meanwhile, piperine also inhibited the PI3K/Akt/mTOR pathway to induce apoptosis in human oral cancer cells (HSC-3). Furthermore, piperine induced autophagy as indicated by increased Beclin-1 expression and LC3-II accumulation in HSC-3 cells. These effects were further support in an HSC-3 xenograft mouse model, where piperine suppressed tumor growth. Xia et al.⁴⁹ reported that piperine induced autophagy-dependent cell death in colorectal cancer (CRC) cells by increasing ROS production and inhibiting Akt/mTOR signaling. *In vivo*, piperine also suppressed tumor growth in a xenograft model of CT26 cell line at a dosage of 20 mg/kg.

5.2 Anti-angiogenesis

Angiogenesis is a key hallmark of tumor progression, as it is required to supply sufficient oxygen and nutrients to support cancer cells survival and migration, leading to metastasis.²⁰ Doucette et al.⁵⁰ demonstrated that piperine inhibited human umbilical vein endothelial cells (HUVECs) proliferation without obvious cytotoxicity. Besides, piperine suppressed HUVECs migration and tube formation *in vitro* and inhibited collagen-induced angiogenesis *ex vivo* in a rat aorta angiogenesis model. Further, piperine reduced MDA-MB-231-induced angiogenesis in the chicken embryo chorioallantois membrane (CAM) model. Li et al.⁵¹ reported piperine inhibited angiogenesis in EA.hy926 endothelial cells induced by lithocholic acid (LCA)-stimulated HCT-116 cells, which occurred through blocking interleukin-8 (IL-8) expression via the Src/epidermal growth factor receptor (EGFR)/ROS-mediated ERK1/2 and Akt signaling pathways. Senrunga et al.⁵² also showed piperine suppressed glioblastoma multiforme (GBM)-induced angiogenesis in a chick CAM U87 glioblastoma xenograft model, accompanied by downregulated

vascular endothelial growth factor A (VEGF-A) and VEGF receptor-2 (VEGFR-2) expression. DOI: 10.1039/D6MD00223D

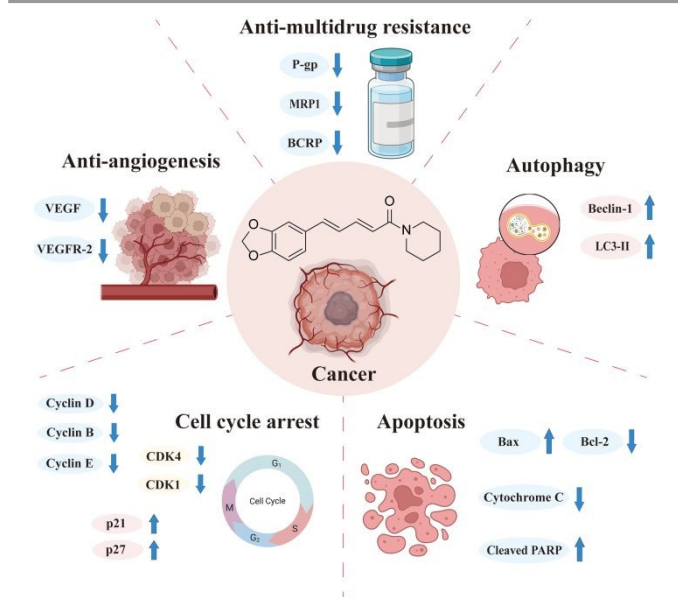


Fig. 4 Anticancer activities of piperine *in vitro*, ↓down-regulated protein targets/markers; ↑up-regulated protein targets/markers. (figure was created with BioRender.com)

5.3 Anti-multidrug resistance

Multidrug resistance (MDR) impairs the anticancer efficacy of chemotherapy by reducing the intracellular accumulation of chemotherapeutic drugs in cancer cells through the overexpression of MDR related proteins.^{53, 54} Piperine could be used in combination with chemotherapeutic agents to reverse MDR and thereby enhance anticancer efficacy. Li et al.⁴⁵ reported that piperine inhibited P-glycoprotein (P-gp), multidrug resistance-associated protein 1 (MRP1) and breast cancer resistance protein (BCRP) expression, which was associated with resensitization to doxorubicin (DOX) and mitoxantrone in resistant cell models, including MCF-7/DOX and A549/cisplatin, respectively. Xu et al.⁵⁵ also reported piperine inhibited MDR1 expression to decrease P-gp protein in 4T1 cells while enhancing the intracellular accumulation of paclitaxel (PTX), thereby increasing the cell sensitivity to PTX.

5.4 Targets of piperine

The anticancer profiles summarized above indicate that piperine affects several cancer-relevant processes, including cell-cycle progression, apoptosis, autophagy, angiogenesis, and multidrug resistance. However, most reported anticancer effects of piperine are associated with multi-pathway modulation, whereas direct molecular target validation and structural information on piperine-target interactions remain limited.

Dihydroorotate dehydrogenase (DHODH) represents one of the few molecular targets of piperine with direct structural validation. Several studies showed that DHODH has emerged as a cancer-relevant metabolic target due to its essential roles in mitochondrial redox regulation and ferroptosis.^{56, 57} Zhang et al.⁵⁸ reported that piperine exhibited inhibitory activity against *h*DHODH ($IC_{50} = 1.73 \mu M$) as an *h*DHODH inhibitor with



anticancer effects. Liu et al.⁵⁹ also identified piperine as a potent inhibitor of *h*DHODH with an IC_{50} value of 0.88 μ M. Further enzymatic kinetic analysis showed that piperine exhibited high inhibitory affinity for *h*DHODH, with an inhibitory constant (K_i) of 0.71 μ M and a long residence time (RT) of 182.95 min. Direct binding of piperine to *h*DHODH was further supported by CD spectroscopy, intrinsic fluorescence quenching, and isothermal titration calorimetry (ITC), with a dissociation constant (K_D) of 1.97 ± 0.20 μ M. The crystal structure of *h*DHODH-piperine complex showed the 1,3-benzodioxole ring is positioned in the hydrophobic region of the channel, whereas the carbonyl oxygen forms a hydrogen bond with Tyr356. Therefore, this study provides valuable structural information for piperine-target binding. In addition, MDR-associated ABC transporters, especially P-gp, were regarded as functional targets involved in the chemosensitizing effect of piperine.⁴⁵

Collectively, piperine has impacts on multiple cancer-relevant processes, including cell-cycle arrest, apoptosis, autophagy, angiogenesis, and drug-resistance pathways. However, most proposed anticancer mechanisms are currently supported by pathway-level observations or biomarker evidence rather than definitive target engagement. In this context, the introduction of target-relevant pharmacophores into piperine derivatives has been used as a strategy to enhance biological potency and achieve more clearly defined target-associated activity.

6. Structural modification and improved anticancer activities

Despite its promising anticancer potential, the clinical application of piperine is hindered by limitations, such as poor aqueous solubility, low bioavailability, and potential toxicity at high-dose exposure. Accordingly, medicinal chemistry studies have focused on structural modification of piperine to optimize its physicochemical and pharmacological properties, improve target engagement, and translate these improvements into enhanced anticancer activity. In most reported derivatives, structural modification has mainly been performed at the amide terminus and its adjacent linker, whereas the 1,3-benzodioxole moiety is retained as an important aromatic moiety. Overall, piperine derivatization can be grouped into three main strategies: polarity/ionizability-related modifications, target-oriented terminal pharmacophore modifications, and linker length/unsaturation/scaffold-rigidity modulation. This section summarizes the representative piperine derivatives within these categories emphasizing changes in biological potency and mechanism-associated phenotypic profiles.

6.1 Polarity/ionizability-related modifications

To address the physicochemical limitation of piperine, several studies have introduced polar or ionizable moieties into the piperine scaffold. In this part, amino acid residues, peptide-like fragments, cyclic dipeptides, and salt-forming groups have been explored to modulate polarity or hydrophilicity with improved cytotoxicity or additional mechanism-related anticancer phenotypes.

Umadevi et al.⁶⁰ synthesized piperine amino acid derivatives **34-36** (Fig.5) via hydrolysis, acylation, and condensation with amine, and then these derivatives were evaluated for their cytotoxic activity in two human cancer cell lines (MCF-7 and HeLa). All compounds demonstrated over 50% inhibition against MCF-7 and HeLa cell lines at approximately 1 μ M. Among them, compound **34**, a histidine-derived analogue bearing an imidazole side chain, exhibited the highest activity against MCF-7 cell line with an IC_{50} value of 0.74 μ M. Similarly, compound **36**, a tryptophan-derived analogue featuring an indole moiety, showed the highest growth inhibition against HeLa cell lines ($IC_{50} = 0.74$ μ M). These results suggest that amino acid conjugation may improve polarity-related properties and contribute to enhanced cytotoxicity for this series.

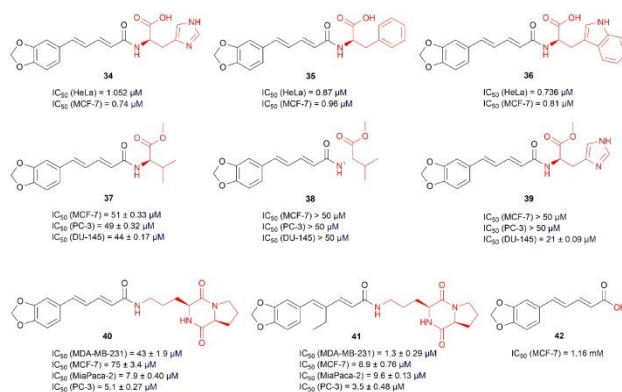


Fig. 5 The chemical structures and anticancer activities of piperine derivatives **34-42**.

Based on the polarity-oriented strategy, Rao et al.⁶¹ further synthesized a series of piperine-amino acid ester conjugates by replacing the parent amide linkage with a peptide-like bond (-CO-NH-). They evaluated the *in vitro* anticancer activity by MTT assay with various cancer cell lines (MCF-7, PC-3, and DU-145) (Fig. 5). The amino acids ester derivatives, including L-valine (**37**, with IC_{50} values of 51.00, 49.00, and 44.00 μ M against MCF-7, PC-3, and DU-145 cell lines, respectively), exhibited better cytotoxic activity than the parent compound piperine with IC_{50} value > 50.00 μ M in the same cell lines. In addition, conjugation of L-amino acids to piperine generally may enhance anticancer activity compared to that of their D-amino acid counterparts (e.g., L-valine analogue **37** vs D-valine analogue **38**). Notably, the heterocyclic side chain-bearing derivative, such as L-histidine derived analogue **39**, was among the most active, with an IC_{50} of 21.00 μ M in DU-145 cells. These findings indicated that amino acid ester conjugation, particularly with heteroaromatic side chain, can enhance the cytotoxicity of piperine derivatives.

A related peptide-based approach was reported by Sudha et al.⁶², who generated four novel piperine derivatives by coupling cyclic dipeptides with piperic acid or 4-ethylpiperic acid scaffolds. Compound **40**, piperic acid-cyclic dipeptides c(Orn-Pro), exhibited better cytotoxicity with IC_{50} value of 7.90 μ M against the MiaPaca-2 cell line. Importantly, compound **41**, 4-ethylpiperic acid-c(Orn-Pro), showed potential cytotoxic activity with IC_{50} 1.30 μ M in MDA-MB-231, 3.50 μ M in PC-3, 8.90



μM in MCF-7, and $9.60 \mu\text{M}$ in MiaPaCa-2 cell lines. Moreover, compound **41** increased E-cadherin while decreasing key mesenchymal markers (Snail, Twist-1, Vimentin) and metastasis-related proteins (MMP2, MMP9) to attenuate MDM2-dependent cancer cell metastasis in a p53-independent manner. In the 4T1 mouse xenograft tumor model, compound **41** significantly reduced both the primary tumor weight by 52% and the tumor volume by 65%, while also inhibiting lung metastasis of cancer cells at a safe and tolerable dosage of 20 mg/kg. Thus, cyclic dipeptide incorporation may not only improve cytotoxic potency but also contribute to anti-metastatic phenotypes.

In addition to amino acid and cyclic dipeptide conjugation, salt formation provides another way to introduce ionizability into piperine-related derivatives. Fan et al.⁶³ demonstrated that the potassium piperonate (GBK) **42** (Fig. 5), as an ionized salt form derived from piperic acid, showed cytotoxic activity against MCF-7 cells with an IC_{50} value of 1.16 mM. The further mechanistic studies showed the GBK inhibited the proliferation of breast cancer cells by arresting the G1/S phase transition via the upregulation of p27 expression and the inhibition of cyclin A, cyclin E, cyclin B expression. In addition, GBK induced apoptosis via the activation of caspase 6 and caspase 9, and the engagement of the p38/JNK MAPK signaling pathways in MCF-7 cells. *In vitro*, the combination of GBK with etoposide phosphate (VP-16) or cisplatin at Sub- IC_{50} concentrations exerted a synergistic inhibitory effect on the viability of MCF-7 cells. In NOD/SCID mice bearing MCF-7 xenografts, intraperitoneal administration of GBK at 10 mg/kg showed significant antitumor efficacy, without an obvious change in body weight. Moreover, their group⁶⁴ further elucidated that **42** downregulated miR-31-associated pro-metastatic genes, such as *SATB2*, *RHOA*, and *WAVE3*, which was consistent with reduced migration and invasion in SUM-159 and MCF-7 cell lines. In addition, the combination of GBK and cisplatin displayed synergistic anticancer activity against SUM-159 cells in the xenograft model.

Overall, amino acid conjugation, cyclic dipeptide incorporation, and potassium salt formation demonstrate that polarity/ionizability-oriented modification is a useful strategy to improve the anticancer potential of piperine derivatives while retaining the benzodioxole-containing parent scaffold.

6.2 Target-oriented terminal pharmacophore modifications

Compared with polarity-oriented strategies, modification of the amide terminus with target-relevant pharmacophores can introduce target-recognition or mechanism-associated structural fragments into the piperine scaffold, thereby enhancing enzyme inhibition, kinase inhibition, MDR reversal, anti-angiogenic activity, or cytotoxic potency.

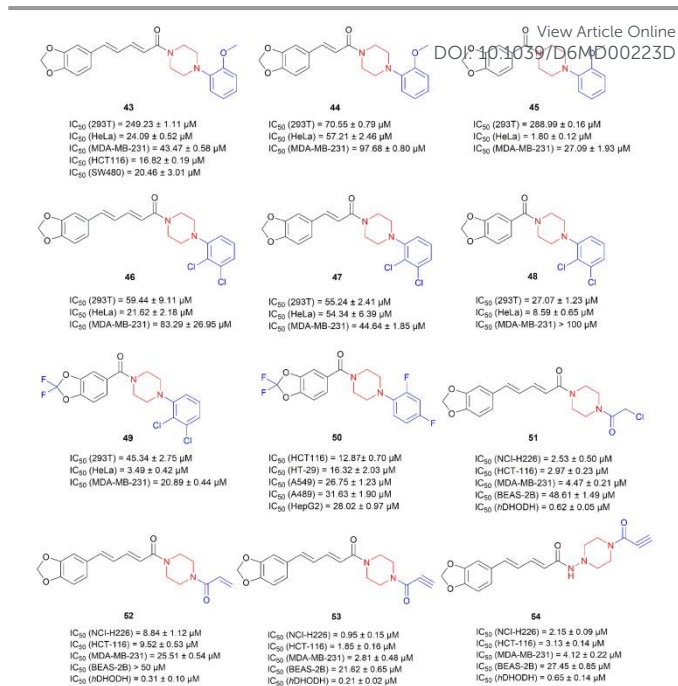


Fig. 6 The chemical structures and anticancer activities of piperine derivatives **43-54**.

As a terminal modification strategy, Wang group⁶⁵ replaced the piperidine moiety of piperine with aryl-piperazine fragments to generate a series of aryl-piperazine-containing piperine derivatives **43-45** (Fig. 6) and further evaluated their anticancer activity in HeLa and MDA-MB-231 cancer cell lines, as well as Human Embryonic Kidney (HEK) 293T normal cells, by MTT assay. As shown in Fig. 6, compound **43**, which retained the piperine scaffold but replaced piperidine with 2-methoxyphenylpiperazine, demonstrated good cytotoxicity against HeLa cells, surpassing that of both 5-fluorouracil (5-FU) (IC_{50} = 44.58 μM) and piperine (IC_{50} = 44.37 μM), while exhibiting relatively low cytotoxicity to HEK293T normal cells. In addition, Zhang group⁶⁶ prepared compound **43** by coupling piperic acid with 1-(2-methoxyphenyl) piperazine and tested its anticancer effects. Compound **43** suppressed colony formation and DNA synthesis in HCT-116 and SW-480 cells. In the CAM xenograft model, it also inhibited HCT116 and SW480 tumor growth and angiogenesis in a dose-dependent manner. Mechanistically, compound **43** impeded tumor progression via activating the p53-dependent apoptosis pathway, while it suppressed the Wnt/ β -catenin signaling pathway to downregulate the expression of β -catenin and cyclin D1 and thereby inhibiting cell proliferation. These findings suggest that the replacement of the piperidine terminus with an aryl-piperazine moiety is an effective terminal modification strategy for enhancing the anticancer profiles of piperine derivatives. Analogues from the same aryl-piperazine series that further involve the linker length or unsaturation modulation, such as **44-50**, are discussed separately below in the Section 6.3.

Zhang et al.⁵⁸ further designed and synthesized piperazine-containing piperine analogues **51-54** (Fig. 6) and subsequent pharmacological assays revealed that these compounds exhibited low IC_{50} values against cancer cell lines. Both



chloroacetamide **51** and propargylamide **53** were more potent in NCI-H226, HCT-116, and MDA-MB-231 cell lines with the IC₅₀ values of 2.53 μM, 2.97 μM, and 4.77 μM for **51** and 0.95 μM, 1.85 μM, and 2.81 μM for **53**, than piperine (IC₅₀ > 50 μM). SAR studies indicated that introducing an electrophilic ethynyl group (-C≡CH) on a piperazine-linked scaffold was advantageous for improving cytotoxicity. Notably, compound **53** was the most potent human dihydroorotate dehydrogenase (*h*DHODH) inhibitor with an IC₅₀ value of 0.21 μM, approximately ten-fold more potent than piperine (IC₅₀ = 1.73 μM). In addition, the calculated aqueous solubility (cLogS = -3.5) and calculated logarithm of the octanol-water partition coefficient (cLogP = 1.6) of **53** were improved compared with piperine (cLogS = -3.9 and cLogP = 3.3). Further, compound **53** inhibited NCI-H226 cells proliferation by inducing ferroptosis, as indicated by the changes in lipid peroxidation level, Fe²⁺, glutathione, and 4-HNE. Molecular docking studies suggested that the carbonyl group adjacent to the ethynyl group formed two direct hydrogen bonds with Arg 136 and Gln 47, while another carbonyl group interacted with Tyr 356, indicating the stabilization of the binding of compound **53** to *h*DHODH.

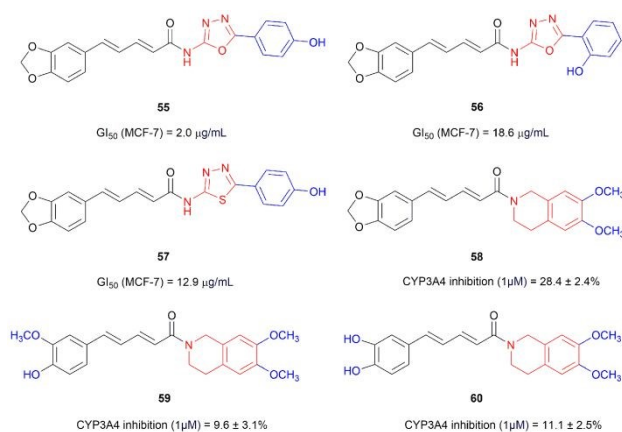


Fig. 7 The chemical structures and anticancer activities of piperine derivatives **55-60**.

Beyond the piperazine-based terminal modification, aryl-heterocyclic moieties have also been incorporated into the piperine scaffold. Amperayani et al.⁶⁷ designed and synthesized new piperine-oxadiazole and thiadiazole analogs **55-57** (Fig. 7) by coupling amino-substituted oxadiazoles/thiadiazoles with piperic acid through an amide linkage. Among these derivatives, the piperine derivative **55** bearing an oxadiazole moiety with a *para*-hydroxyl group exhibited the highest antiproliferative activity against MCF-7 cells, with a 50% growth inhibition (GI₅₀) value of 2.00 μg/mL, which was more potent than piperine (GI₅₀ = 11.72 μg/mL), suggesting that the electron-donating hydroxyl substituent was beneficial for antiproliferative activity. Docking studies indicated that compound **55** was docked into the 3EU7 protein pocket, where it was surrounded by the residues of Val-200, Tyr-300, Ala-278, and Phe-300, and formed stable hydrogen bonds. They attributed these interactions to the rigid scaffold of **55** with an amide linkage and hydroxyl groups on heterocyclic moiety, with low binding energy of -15.23 kcal/mol.

Terminal pharmacophore hybridization has also been applied to overcome multidrug resistance. Syed and co-workers⁶⁸ synthesized piperine hybrid as P-gp inhibitors for overcoming multidrug resistance. In the earlier study, the piperic acid with 6, 7-dimethoxytetrahydroisoquinoline hybrid **58** (Fig. 7) incorporating a moiety derived from the P-glycoprotein inhibitor elacridar, reversed drug resistance to the chemotherapeutic agents (vincristine, colchicine, and paclitaxel) in P-gp-overexpressing KB and SW480 cancer resistant cells and outperformed the parent piperine. Further studies demonstrated that compound **58** enhanced the intracellular concentration of these chemotherapeutic drugs in resistant cells by inhibiting P-gp-mediated efflux. Additionally, methoxy substitution was identified as a key group of P-gp inhibitory activity.⁶⁸ Syed group⁶⁹ subsequently designed analogues **59-60** (Fig. 7) based on compound **58** via the ring-opening of dioxole moiety and methylation. Compound **59** reversed vincristine resistance in KB Ch^R 8-5 cells and was identified as a promising P-gp inhibitor with low CYP3A4 inhibitory activity. It also potentiated the vincristine-induced apoptosis which is mediated by NF-κB pathway.

In addition to heterocyclic groups, terminal aromatic structural modifications are associated with redox regulation and epigenetic enzyme inhibition. Zhong et al.⁷⁰ reported two series of piperine-benzene derivatives and tested their cytotoxicity against four cancer cell lines, HeLa, HepG2, SMMC-7721, and A549. As shown in Fig. 8, compound **61**, which was derived from the incorporation of a meta-chlorophenyl moiety into the piperine, showed good inhibitory activity with IC₅₀ values in the range of 23-38 μM. Its cytotoxic activity (IC₅₀ = 23.10 μM) in the HeLa cell line was three-fold more than that of the parent compound piperine (IC₅₀ = 85.10 μM). These studies suggested the *meta*-position electron-withdrawing substitution on the appended phenyl ring potentiated cytotoxicity, whereas modulation of the conjugated chain length had no discernible effect within this series. Further investigation revealed that compound **61** selectively inhibited TrxR activity *via* the binding with the Sec residue, disrupted the redox balance by generation of additional ROS levels in the cells, and eventually caused apoptosis of HeLa cells.

Somsakeesit et al.⁷¹ reported the synthesis of piperine derivatives (Fig. 8) via hydrolysis and amidation reactions by coupling piperic acid to 2-aminophenyl (**62**) or 2-hydroxyphenyl (**63**), respectively. Subsequently, the derivatives were evaluated for histone deacetylase (HDAC) inhibition and for cytotoxic activity against the HeLa cell line by MTT assay. Compound **62** and **63** inhibited HDAC with IC₅₀ values of 85.61 μM and 111.27 μM, respectively, outperforming piperine (IC₅₀ = 352.80 μM). In addition, compound **63** showed potent cytotoxic activity against HeLa cells with IC₅₀ value of 10.38 μg/mL. Further docking studies suggested that compound **62/63** could form hydrogen bond toward HDAC active site and chelated with Zn²⁺ binding site. The hydroxyl and amino groups were proposed to enhance hydrogen bond formation, whereas the phenyl ring may contribute to hydrophobic interactions and π-π stacking interactions. In addition, their group⁷² further reported the anticancer activity of **63** against MCF-7 cells by cytotoxic assays



with IC_{50} values $17.02 \mu\text{g/mL}$. Further studies demonstrated that compound **63** increased the level of intracellular reactive oxygen species (ROS) and induced apoptosis involving the modulation of DNA repair, estrogen receptor- α (ER- α), and PI3K/Akt pathways.

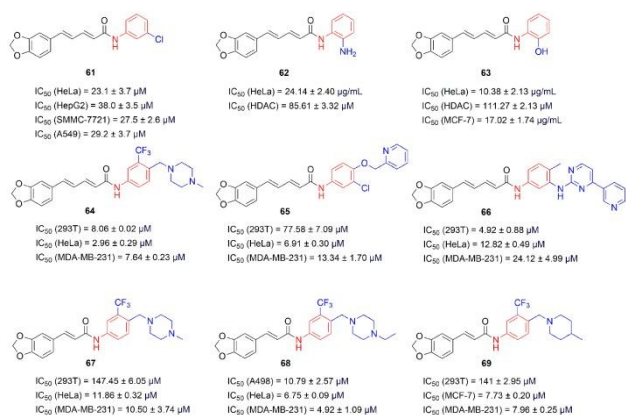


Fig. 8 The chemical structures and anticancer activities of piperine derivatives 61-69.

As shown in Fig. 8, Wang et al.⁷³ synthesized piperine derivatives **64-67** by modifying the piperidine part and using a fragment-splicing strategy, in which kinase inhibitory fragments (structural motifs derived from imatinib, neratinib, and ponatinib) were conjugated to the piperine scaffold *via* acyl chloride-mediated amidation. The cytotoxic effect of the modified compounds against HeLa cells was higher than that of the parent compound of piperine ($IC_{50} = 44.37 \mu\text{M}$) and the positive control drug 5-FU ($IC_{50} = 44.58 \mu\text{M}$), and their IC_{50} values were mainly in the range of 3-13 μM . Though compound **64** showed the best cytotoxic effect against HeLa and MDA-MB-231 cell lines, it exhibited a lower IC_{50} value (8.06 μM) against HEK293T cell line, indicating its toxicity towards normal cells. These findings suggest that the replacement of the piperidine terminus with kinase inhibitory fragment is also a useful strategy for enhancing the anticancer profiles of piperine derivatives. Related analogues in this series that additionally modulate the linker length or unsaturation, such as **67-69**, are discussed separately in the Section 6.3.

Terminal urea and sulfonamide pharmacophores can transform piperine derivatives into target-oriented enzyme or receptor kinase inhibitors. Elimam et al.⁷⁴ designed and synthesized a series of piperine-urea derivatives as carbonic anhydrase inhibitors (CAIs) by integrating a benzenesulfonamide fragment inspired by SLC-0111 (a selective *hCA* IX inhibitor) onto the piperine skeleton. These compounds were investigated against four human carbonic anhydrases (*hCA*) isoforms to confirm isoform selectivity. Among the tested compounds, the primary sulfonamido zinc-binding group (ZBG) analogues **70** and **71** (Fig. 9) displayed potent inhibitory activity against *hCA* IX (inhibition constants (K_i) = 38.7 nM and 68.2 nM, respectively) and *hCA* XII (K_i) = 57.5 nM and 45.6 nM, respectively). Extending the urea linker of the *para*-regioisomer **70** by inserting an ethylene spacer (**71**) increased inhibition of *hCA* I, II and XII, but reduced *hCA* IX potency, indicating that

linker length tunes isoform preference. Furthermore, compound **70** exhibited significant cytotoxic activity against the MCF-7 cancer cell line with IC_{50} of 2.17 μM , superior to reference drug staurosporine ($IC_{50} = 4.10 \mu\text{M}$). Moreover, compound **70** increased the Sub-G1 fraction and decreased the G2/M population compared to the untreated control. SAR studies⁷⁴ revealed that incorporation of a primary sulfonamido moiety as a ZBG on the terminal phenyl ring and introduction of a urea linker appear to enhance *hCA* IX/ XII engagement, consistent with the improved activity towards MCF-7 cells.

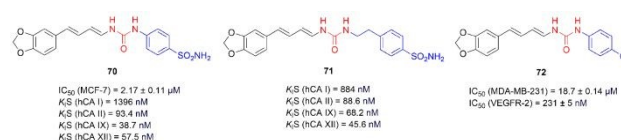


Fig. 9 The chemical structures and anticancer activities of piperine derivatives 70-72.

In a follow-up study, Elimam and co-workers⁷⁵ expanded the urea-based piperine derivatives and evaluated these derivatives against three human cancer cell lines by the MTT assay. Compound **72** (Fig. 9), featuring a *para*-chloro-substituted benzene moiety on the urea terminus, emerged as the most potent anticancer analogue against MDA-MB-231 cells with IC_{50} value of 18.70 μM , improving on piperine ($IC_{50} = 47.80 \mu\text{M}$) and 5-FU ($IC_{50} = 38.50 \mu\text{M}$). Moreover, compound **72** induced apoptosis through G2/M phase cell cycle arrest and halted DNA synthesis via reduction in the S-phase cell population. Further studies showed that compound **72** inhibited the VEGFR-2 with $IC_{50} = 231 \text{ nM}$ in the VEGFR-2 enzymatic assay. Molecular docking studies indicated that **72** could dock into the ATP-binding site of VEGFR-2, and the piperine skeleton formed a key H-bond with Cys919, while the urea carbonyl oxygen and the urea linker engaged Glu885 and Asp1046 via additional H-bond interactions to achieve good VEGFR-2 inhibition.

The incorporation of hydrazone or acylhydrazone moieties provides an approach to introduce hydrogen-bonding and aromatic pharmacophore features into piperine. Tantawy group⁷⁶ reported the preparation of a series of novel piperine-hydrazone hybrids with resveratrol-like phenolic pharmacophore moieties *via* hydrolysis, acylation, and conjugation reactions. The cytotoxic activity of the target compounds was examined against sixty cancer cell lines of nine different tissues at single concentration of 10 μM . The experimental results showed compound **73-75** (Fig. 10) had significant cytotoxic activity. Particularly, compound **73**, possessing a resveratrol pharmacophoric phenolic moiety, showed 91% and 85% growth inhibition in HCT-116 and MCF-7 cells, respectively. Moreover, compounds **73-75** exhibited higher percent inhibition of SIRT2 than SIRT1 at 50 μM . Notably, compound **73** inhibited the SIRT2 enzyme with an IC_{50} value of 21 μM and induced G1-phase cell cycle arrest in MCF-7 cancer cells.



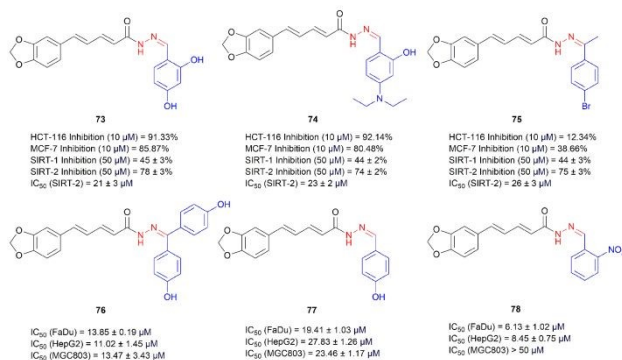


Fig. 10 The chemical structures and anticancer activities of piperine derivatives **73-78**.

In 2024, Xu et al.⁷⁷ synthesized a series of novel piperine-hydrazone hybrids **76-78** (Fig. 10) and evaluated their anti-proliferative activities in FaDu, HepG2, and MGC803 cells. Compound **76** exhibited significant inhibitory activity against FaDu, HepG2, and MGC803 cells with IC₅₀ values of 13.85, 11.02, and 13.47 μ M, respectively. In addition, compound **78**, a *meta*-nitro-substituted benzoyl acylhydrazone analogue in this series, exhibited the strongest cytotoxic activity against FaDu and HepG2 with IC₅₀ values of 6.13 and 8.45 μ M, respectively.

As another example of target-oriented terminal modification, Al-Wahaibi et al.⁷⁸ developed a series of piperine-carboximidamide hybrids from piperine via hydrolysis followed by amidation, and then evaluated them against several protein kinases and cancer cell lines. Among them, compounds **79-82** (Fig. 11) effectively inhibited A549, MCF-7, HT-29, and PANC-1 cell growth, with IC₅₀ values ranging from 32 to 55 nM, and also showed potent inhibitory effects on EGFR, BRAF^{V600E}, and CDK2 kinases with IC₅₀ values from 12 to 127 nM. Compounds **79-81** also demonstrated promising cytotoxic activity against LOX-IMVI melanoma cells with IC₅₀ values ranging from 1.05 to 1.40 μ M. Notably, compound **79**, bearing a 1,3-benzodioxole moiety, emerged as the most potent derivative, exhibiting the lowest IC₅₀ values. It inhibited MCF-7 cells with an IC₅₀ value of 35 nM, outperforming erlotinib (40 nM). Meanwhile, compound **79** also showed the strongest inhibitory activity against CDK2 (IC₅₀ = 12 nM), which was 1.7-fold more potent than dinaciclib (IC₅₀ = 20 nM). This study indicates that aryl carboximidamide incorporation is a useful strategy for developing piperine-based hybrids with kinase-inhibitory anticancer activity.

Taken together, target-oriented terminal pharmacophore modification provides a viable strategy to convert piperine, an active natural product scaffold, into derivatives with improved target selectivity against hDHODH, P-gp, TrxR, HDAC, hCA, VEGFR-2, SIRT2, EGFR, BRAF^{V600E}, and CDK2.

6.3 Linker length, unsaturation, and scaffold-rigidity modulation

This section focuses on the modulation of linker length, unsaturation degree, and scaffold rigidity. The conjugated diene linker of piperine connects the 1,3-benzodioxole aromatic region to the terminal amide moiety and can affect the electronic distribution and molecular stability.^{73, 79} Therefore, structural modification of this unsaturated linker can alter cytotoxic potency and anticancer phenotypes.

Within the aryl-piperazine series, modifications to the unsaturated linker affect anticancer activity. Compared with compound **43**, compound **45** (Fig. 6), which lacks the conjugated unsaturated chain, exhibited the highest potency against HeLa cells (IC₅₀ = 1.8 μ M) while displaying low cytotoxicity to HEK293T normal cells (IC₅₀ = 288.99 μ M). Compound **45** also inhibited colony formation, migration, and adhesion of HeLa cells, and suppressed tumor growth and neovascularization in a HeLa xenograft chick embryo model.

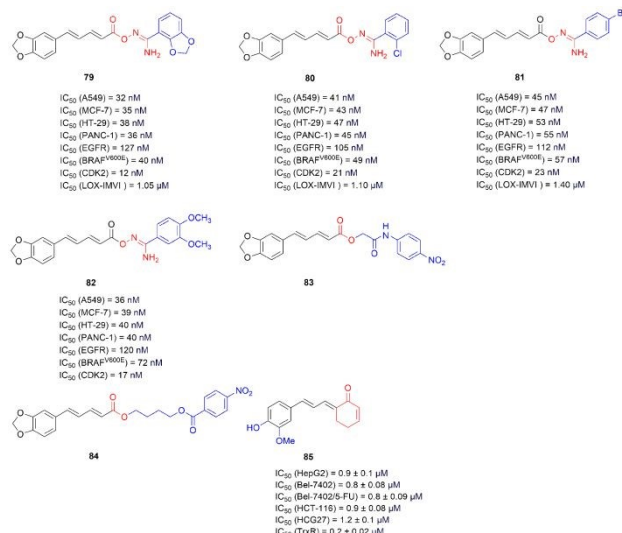


Fig. 11 The chemical structures and anticancer activities of piperine derivatives **79-85**.

Wang group⁸⁰ also synthesized the aryl-piperazine analogues **46-49** (Fig. 6) and evaluated their anticancer activity. Compound **49** displayed IC₅₀ values of 45.34 μ M in HEK293T normal cell line, 3.49 μ M in HeLa cell line, and 20.89 μ M in MDA-MB-231 cell line, which was better than the 5-FU and piperine, indicating potent anticancer efficacy with relatively low toxicity. Moreover, compared with compound **46**, compound **49** featured a shortened unsaturated linker and fluorination on the benzodioxole moiety, and inhibited proliferation, adhesion and invasion of HeLa cell *in vitro*. In the chicken embryo model, compound **49** significantly inhibited tube formation and suppressed the growth of HeLa xenograft tumors at a dosage of 10 μ g/ μ L. SAR analysis⁶⁵ suggested that shortening the unsaturated chain and replacing the piperidine with an aryl-piperazine motif improves *in vitro* potency.

In addition, Zhang group⁸¹ reported that aryl-piperazine derivative **50** (Fig. 6) showed potent cytotoxic activity against colon cancer cells with IC₅₀ values of 12.87 μ M (HCT116) and 16.32 μ M (HT-29), significantly lower than those of parent piperine (45.62 and 41.32 μ M, respectively). Mechanistically, compound **50** downregulated Mki67 expression and activated the p53 pathway, inhibited the E2F pathway, and reduced colorectal cancer cell proliferation, migration, invasion, and angiogenesis in both cell-based and chicken embryo models. These findings suggest that the combination of terminal aryl-piperazine substitution and linker modulation can enhance the anticancer potency.



Within the 1,3-benzodioxole-containing series, linker length and degree of unsaturation have also been explored. Compared with compound **64**, compound **67** (Fig. 8) featured a shortened conjugated unsaturated linker and showed markedly reduced cytotoxicity toward HEK293T normal cells, with an approximately 18-fold lower IC_{50} value (147.45 μ M vs 8.06 μ M for **64**), indicating higher selective inhibition (SI) to cancer cells of both HeLa (IC_{50} = 11.86 μ M) and MDA-MB-231 (IC_{50} = 10.50 μ M). Further biological evaluation exhibited that compound **67** inhibited the proliferation, migration, and adhesion of HeLa cells *in vitro*, and significantly suppressed tumor angiogenesis and reduced tumor weight in a chicken embryo model *in vivo*. Moreover, their group⁸² designed a series of 1,3-benzodioxole derivatives (a core moiety of piperine essential for antitumor activity) by retaining the 1,3-benzodioxole ring, introducing a vinyl linker and incorporating trifluoromethylpiperazine. Further pharmacological evaluation confirmed that compound **68**, bearing a *para*-ethyl substituent on the aryl-piperazine, showed improved cytotoxic activity against MDA-MB-231 cells (IC_{50} = 4.92 μ M) in comparison with 5-FU (IC_{50} = 18.06 μ M) and piperine (IC_{50} = 239.03 μ M), consistent with *para*-electron-donating substitution as a favorable handle in this series. It also inhibited tumor angiogenesis and reduced tumor volume and weight without affecting chick embryo weight in CAM xenograft models. SAR studies^{73, 82} indicated that this compound, obtained by replacing the piperidine moiety of piperine with an amine side chain containing a trifluoromethyl piperazine moiety and bearing a *para*-substituted electron-donating group on the piperazine ring, may exhibit potent antitumor activity. Additionally, a vinyl linker connecting benzodioxole core to amide region appeared to be beneficial for improving the anticancer effect in this series.

Zhou group⁷⁹ also synthesized compound **69** (Fig. 8), an analogue of compound **67**. In particular, compound **69** exhibited lower IC_{50} values of 7.73 μ M and 7.96 μ M in MCF-7 and MDA-MB-231 cells, respectively, compared with those (13.15 μ M and 14.40 μ M, respectively) of piperine in the same cell lines. In addition, compound **69** exhibited a reduced cytotoxic effect on HEK293T normal cells (IC_{50} = 141.00 μ M) compared to piperine (IC_{50} = 98.11 μ M). Compound **69** was found to effectively suppress breast cancer cell proliferation, adhesion, invasion, and migration by inducing cell cycle arrest *via* modulation of the p53/p21-CDK4/6-cyclin D-Rb-E2F pathway. In addition, compound **69** promoted apoptosis in breast cancer cells by modulating the Bax/Bcl-2/Caspase 3 signaling pathway. Docking studies indicated that compound **69** binds within the key hydrophobic pockets of MDM2, yielding an AutoDock Vina score of -10.1 kcal/mol, which is consistent with a putative inhibition of MDM2-mediated p53 degradation. These studies proposed that the removing the conjugated C=C segment (direct aryl-amide connection) and introducing a trifluoromethyl-substituted aryl unit could modulate structure electronic properties and lipophilicity, thereby improving target-relevant interactions and cellular phenotypes.^{79, 82}

Ester-linked modification represents another strategy to extend the molecular skeleton of piperine analogues. Santos et al.⁸³ prepared piperine-ester analogue **83** (Fig. 11), N-(*p*-

Nitrophenyl) acetamide piperinoate. They tested its toxicity and then evaluated its anticancer effects in Ehrlich ascites carcinoma (EAC) model. Compound **83** reduced Ehrlich tumor cell viability and peritumoral microvessel density at the dosage of 12.5 mg/kg *in vivo*. Moreover, compound **83** increased the production of reactive oxygen species (ROS) and nitric oxide (NO). Further, their group⁸⁴ synthesized a related analogue **84** (Fig. 11) with an altered linker. Compound **84**, the butyl 4-(4-nitrobenzoate)-piperinoate, showed low acute toxicity, with a lethal concentration 50% (LC_{50}) > 100 μ g/mL by the fish embryo toxicity (FET) assay and a lethal dose 50% (LD_{50}) around 1000 mg/kg (i.p.) in an acute mouse toxicity test. Moreover, compound **84** showed potential antitumor activity in the EAC mice model at 50 mg/kg, which was attributed to modulation of the tumor microenvironment via oxidative stress induction and anti-angiogenic effects.

In addition to the ester-linked analogues, Zhu et al.⁸⁵ designed a series of phenylallylidencyclohexenone hybrids by integrating the aromatic-olefin-lactam motif of piperlongumine with the α , β -unsaturated carbonyl (enone) moiety of piperine, while replacing the lactam ring with a cyclohexanone. The hybrids were evaluated against five human cancer cell lines and showed IC_{50} values in the range from 0.80 to 8.10 μ M, outperforming both the parent piperlongumine and piperine. Among them, compound **85** (Fig. 11) exerted the most potent cytotoxic activity against drug-resistant Bel-7402/5-FU human liver cancer cells with an IC_{50} value of 0.80 μ M and low cytotoxicity towards LO2 human normal liver epithelial cells. Meanwhile, the enzymatic activity of TrxR was significantly inhibited by **85**, with an IC_{50} value of 0.20 μ M. Mechanistically, compound **85** induced autophagy, accompanied by p38 activation, suppression of the Akt/mTOR signaling pathway, and modulation of LC3, p62 and Beclin-1 proteins.

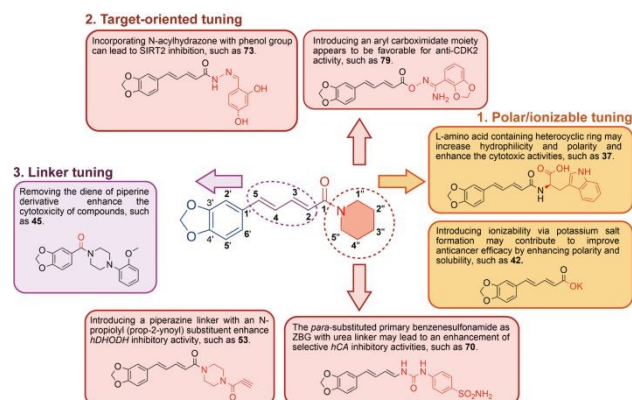


Fig. 12 Graphical depiction of the structure-activity relationship of piperine derivatives for the anticancer activity.

To sum up, the effects of piperine and its derivatives on the target proteins were presented in Table 2. As shown, piperine derivatives not only displayed strong inhibitory effect on hDHODH, but also showed potential inhibition of other targets, including hCA, SIRT-2, and TrxR. Notably, the aryl carboximidamide derivative **79** exhibited excellent inhibitory activity against CDK2, as well as additional target proteins, such as EGFR, and BRAF^{V600E}.



Table 2 Effects of piperine and its derivatives on the target proteins.

Compound	Proteins	IC ₅₀	Reference
1 (piperine)	<i>hDHODH</i>	0.88 μM, 1.73 μM	[58, 59]
53	<i>hDHODH</i>	0.21 μM	[58]
62	HDAC	85.61 μM	[71]
70	<i>hCA IX</i>	38.7 nM	[74]
71	<i>hCA XII</i>	45.6 nM	[74]
72	VEGFR-2	231 nM	[75]
73	SIRT-2	21 μM	[76]
79	EGFR, BRAF ^{V600E} , CDK2	127 nM, 40 nM, 12 nM	[78]
85	TrxR	0.20 μM	[85]

Based on the cancer-related pharmacological activities of piperine derivatives reported above, the structure-activity relationships (SARs) of piperine derivatives were analyzed and summarized in order to gain insights into rational optimization of piperine. Firstly, the incorporation of polarity/ionizability-related moieties into piperine, while retaining the 1,3-benzodioxole aromatic moiety, appears to enhance its anticancer efficacy. Notably, the amino acid conjugation serves as an effective method for tuning polarity of piperine derivatives. The introduction of L-amino acids, especially heteroaromatic amino acids (e.g., histidine **34** or tryptophan **36**) could improve solubility and modulate hydrophilicity, thereby contributing to enhanced cytotoxicity. In addition, the conversion to the potassium salt **42** introduces ionizability and increases polarity, which may improve aqueous solubility and thereby contribute to anticancer efficacy. Secondly, beyond optimizing physicochemical properties, the piperine scaffold can be modified at the amide terminus with target-relevant pharmacophores to generate piperine hybrids with target selectivity. Mechanistically, terminal pharmacophore cooperation can either strengthen the intrinsic target engagement of piperine or introduce the target-binding moiety, thereby optimizing binding interactions and ultimately enhancing its anticancer activity. Specifically, the terminal introduction of the piperazine linker, followed by the N-propargyl (prop-2-ynoyl) group as an electrophilic motif, contributes to enhancing the *hDHODH*-targeted inhibition of piperine (e.g., **53**). The substitution of a *para*-primary benzenesulfonamide Zn²⁺-binding moiety via a urea linker also affords selective inhibition against *hCA* isoforms, while the linker spacer length further modulates isoform selectivity (e.g., **70/71**). In addition, the conversion of the terminal amide to an (acyl)hydrazone linkage with phenolic pharmacophore hybridization contributes to SIRT2 inhibition with enhanced cytotoxicity (e.g., **73**). Moreover, the installation of an aryl carboximidamide moiety in combination with 1,3-benzodioxole moiety, is favorable for the multi-targeted inhibition activity (EGFR, BRAF^{V600E}, CDK2) with strong cytotoxicity (e.g., **79**). Thirdly, tuning the linker length and unsaturation of the aliphatic chain moiety seems to modulate its cytotoxic potency, with linker shortening being favorable in several series. Notably, in aryl-piperazine-modified piperine derivatives, shortening the linker to a single double bond slightly reduces cytotoxicity, whereas removal of the unsaturated diene chain enhances potency (e.g., **45**). Collectively, these findings demonstrate that

both amide terminal modification and aliphatic linker optimization are effective strategies to enhance its anticancer potency while preserving its privileged parent scaffold (Fig. 12).

7. Conclusion and prospect

Piperine, an alkaloid from *Piper nigrum*, is a widely studied natural product scaffold that has shown great potential to motivate extensive structural optimization for anticancer application. This review summarizes the advances (from 2012 to 2025) in the structural characterization, synthesis/biosynthesis, anticancer profile, structural modifications, and structure activity relationship of piperine-derived anticancer agents. Nevertheless, there are still several limitations, highlighting future directions for developing piperine-based derivatives into viable therapeutic options.

(1) Most anticancer-oriented structural modifications of piperine have focused on the piperidine part, whereas the aliphatic olefin chain remains comparatively underexplored. Future work should be paid more attention to elucidate the SAR and anticancer effects associated with modifications to this aliphatic chain region.

(2) Piperine is a multi-target anticancer compound with activity across diverse cancer types. Accordingly, the hybridization of piperine with other anticancer molecules or suitable pharmacophores may generate hybrids with enhanced efficacy, consistent with the strategy of multi-target drug development.

(3) The piperine derivatives can be predicted and designed by Artificial Intelligence (AI)-assisted approaches, based on molecular targets associated with anticancer activity. AI-driven structural optimization can accelerate lead compound refinement, potentially enhancing efficacy while reducing toxicity.⁸⁶ This strategy offers significant promise for the rational design of piperine-based anticancer agents.

(4) Nanoformulation has shown potential to improve drug stability, solubility, and bioavailability.^{87, 88} In addition, co-administration with bioenhancers exhibits great promise in reducing drug resistance and improving drug efficacy.⁸⁹ Exploring innovative approaches for boosting bioavailability properties to enhance the anticancer efficacy of piperine remains a promising direction for future research.

(5) To fully elucidate the anticancer potential of piperine and its derivatives, more *in vivo* investigations are required, as robust *in vitro* potency does not always translate to meaningful efficacy within intact living systems.

It is hoped that this review will be helpful for the ongoing research of piperine, and provide guidance for the advancement of more effective piperine-based anticancer agents.

Conflicts of interest

The authors declare no conflict of interest for this study.



Abbreviations

SAR	Structure activity relationship	MDA-MB-231	Human triple-negative breast cancer cell line
UV	Ultraviolet spectroscopy	MCF-7	Human estrogen receptor-positive breast cancer cell line
NMR	Nuclear magnetic resonance	MiaPaCa-2	Human pancreatic cancer cell line
MS	Mass spectrometry	MMP	Matrix metalloproteinase
IR	Infrared spectroscopy	MDM2	Mouse double minute 2 homolog
CuCN	Copper cyanide	4T1	Murine mammary carcinoma cell line
LiCl	Lithium chloride	HEK293T	Human embryonic kidney 293T cell line
DMP	Dess-Martin periodinane	MTT	3-(4,5-dimethylthiazol-2-yl)-2,5-diphenyltetrazolium bromide
PivOH	Pivalic acid	HCT-116	Human colorectal carcinoma cell line
PAL	Phenylalanine ammonia lyase	SW480	Human colorectal adenocarcinoma cell line
NADPH	Nicotinamide adenine dinucleotide phosphate	5-FU	5-Fluorouracil
SAM	S-Adenosylmethionine	HT-29	Human colon adenocarcinoma cell line
CoA	Coenzyme A	NCI-H226	Human lung squamous cell carcinoma cell line
PLP	Pyridoxal phosphate	hDHODH	Human dihydroorotate dehydrogenase
MDR	Multidrug resistance	cLogS	Calculated logarithm of aqueous solubility
CDK	Cyclin-dependent kinase	cLogP	Calculated logarithm of the octanol-water partition coefficient
Cdc25C	Cell division cycle 25C	Arg	Arginine
MDA-MB-468	Triple-negative human breast carcinoma cell line	Gln	Glutamine
DLD-1	Human colorectal adenocarcinoma cell line	Tyr	Tyrosine
PI3K	Phosphoinositide 3-kinase	GI ₅₀	50% growth inhibition concentration
Akt	Protein kinase B	Val	Valine
ERK	Extracellular signal-regulated kinase	Ala	Alanine
Cyt-c	Cytochrome c	Phe	Phenylalanine
Smac/DIAB	Second mitochondria-derived activator of caspases/direct IAP-binding protein with low pI	NF-κB	Nuclear factor kappa-light-chain-enhancer of activated B cells
LO	Low density lipoprotein	HepG2	Human hepatocellular carcinoma cell line
NOD/SCID	Non-obese diabetic/severe combined immunodeficiency	SMMC-7721	Human hepatocellular carcinoma cell line
Bcl-2	B-cell lymphoma 2	A549	Human lung adenocarcinoma cell line
Bax	Bcl-2-associated X protein	TrxR	Thioredoxin reductase
PARP	Poly (ADP-ribose) polymerase	Sec	Selenocysteine
mTOR	Mechanistic target of rapamycin	HDAC	Histone deacetylase
HSC-3	Human tongue squamous cell carcinoma cell line	CAIs	Carbonic anhydrase inhibitors
LC3-II	Lipidated microtubule-associated protein 1 light chain 3	SLC-0111	A selective human carbonic anhydrase IX inhibitor
ROS	Reactive oxygen species	ZBG	Zinc-binding group
CT26	Murine colon carcinoma cell line	Cys	Cysteine
HUVECs	Human umbilical vein endothelial cells	Glu	Glutamic acid
CAM	Chick embryo chorioallantois membrane	Asp	Aspartic acid
LCA	Lithocholic acid	SIRT	Sirtuin
IL-8	Interleukin-8	FaDu	Human hypopharyngeal squamous cell carcinoma cell line
EGFR	Epidermal growth factor receptor	MGC803	Human gastric carcinoma cell line
GBM	Glioblastoma multiforme	PANC-1	Human pancreatic ductal adenocarcinoma cell line
VEGF-A	Vascular endothelial growth factor A	BRAF	B-Raf proto-oncogene, serine/threonine kinase
VEGFR-2	Vascular endothelial growth factor receptor 2	LOX-IMVI	Human melanoma cell line
P-gp	P-glycoprotein	JNK	c-Jun N-terminal kinase
MRP1	Multidrug resistance-associated protein 1	MAPK	Mitogen-activated protein kinase
BCRP	Breast cancer resistance protein	VP-16	Etoposide
DOX	Doxorubicin	SATB2	Special AT-rich sequence-binding protein 2
PTX	Paclitaxel	RHOA	Ras homolog family member A
HeLa	Human cervical cancer cell line		
PC-3	Human prostate cancer cell line		
DU-145	Human prostate cancer cell line		
IC ₅₀	Half-maximal inhibitory concentration		

DOI: 10.1039/D6MD00223D



WAVE3	Wiskott-Aldrich syndrome protein family verprolin-homologous protein 3
SUM-159	Human breast cancer cell line
EAC	Ehrlich ascites carcinoma
NO	Nitric oxide
LC ₅₀	Median lethal concentration
LD ₅₀	Median lethal dose
FET	Fish embryo toxicity test
i.p.	Intraperitoneal injection
Bel-7402	Human hepatocellular carcinoma cell line
LO2	Human liver cell line
K _i	Inhibitory constant
RT	Residence time
ITC	Isothermal titration calorimetry
K _d	Dissociation constant
SI	Selective inhibition

Acknowledgements

This work was financially supported by the Science and Technology Development Fund, Macau SAR (File no. 0317/2022/A3, 0001/2023/AKP, and 0003/2025/NRP). This work was also funded by Department of Science and Technology of Guangdong Province; Macao Science and Technology Development Fund (Project No.: no. 2025B1212040001 and no. 0002/2025/COP).

References

1. F. Bray, M. Laversanne, H. Sung, J. Ferlay, R. L. Siegel, I. Soerjomataram and A. Jemal, *CA Cancer J Clin*, 2024, **74**, 229–263.
2. M. K. Manickasamy, A. Kumar, B. BharathwajChetty, M. S. Alqahtani, M. Abbas, A. Alqahtani, J. Unnikrishnan, A. Bishayee, G. Sethi and A. B. Kunnumakkara, *Life Sci*, 2024, **354**, 122943.
3. B. E. Wilson, S. Jacob, M. L. Yap, J. Ferlay, F. Bray and M. B. Barton, *Lancet oncol*, 2019, **20**, 769–780.
4. Y. Wang, F. Wang, W. Liu, Y. Geng, Y. Shi, Y. Tian, B. Zhang, Y. Luo and X. Sun, *Pharmacol Ther*, 2024, **264**, 108752.
5. J. T. Traxler, *J. Agric. Food Chem.*, 1971, **19**, 1135–1138.
6. A. Tiwari, K. R. Mahadik and S. Y. Gabhe, *Medicine in Drug Discovery*, 2020, **7**, 100027.
7. H. L. Wiraswati, I. F. Ma'ruf, J. Sharifi-Rad and D. Calina, *Biofactors*, 2025, **51**, e2134.
8. M. Verzele, F. V. Damme and G. Schuddinck, *J. Chromatogr. A*, 1989, **471**, 335–346.
9. P. N. Ravindran and J. A. Kallapurackal, in *Handbook of Herbs and Spices*, ed. K. V. Peter, Woodhead Publishing, England, second edn., 2012, vol. 1, ch. 6, pp. 86–115.
10. S. S. Mishra and J. P. Tewari, *J. Pharm. Sci.*, 1964, **53**, 1423–1424.
11. V. C. Verma, E. Lobkovsky, A. C. Gange, S. K. Singh and S. Prakash, *J Antibiot (Tokyo)*, 2011, **64**, 427–431.
12. H. K. Juliani, A. R. Koroch, L. Giordano, L. Amekuse, S. Koffa, J. A. Dartey and J. E. Simon, in *African Natural Plant Products Volume II: Discoveries and Challenges in Chemistry, Health, and Nutrition*, eds. H. R. Juliani, J. E. Simon and C. T. Ho, American Chemical Society, 2013, vol. 1127, ch. 3, pp. 33–48. DOI: 10.1039/D6MD00223D
13. W. L. Chang, J. Y. Peng, C. L. Hong, P. C. Li, S. M. Chye, F. J. Lu, H. Y. Lin and C. H. Chen, *Antioxidants (Basel)*, 2025, **14**.
14. X. Hu, D. Wu, L. Tang, J. Zhang, Z. Zeng, F. Geng and H. Li, *Food Chem*, 2022, **394**, 133558.
15. Q. N. Baito, H. M. Jaafar and T. A. M. Mohammad, *Cell Immunol*, 2023, **391–392**, 104752.
16. R. Nasrnezhad, S. Halalkhor, F. Sadeghi and F. Pourabdolhossein, *Mol Neurobiol*, 2021, **58**, 5473–5493.
17. J. Ledesma-Aparicio, P. Mailloux-Salinas, D. J. Arias-Chavez, E. Campos-Perez, S. Calixto-Tlacomulco, A. Cruz-Rangel, J. P. Reyes-Grajeda and G. Bravo, *J Biochem Mol Toxicol*, 2024, **38**, e70040.
18. Y. S. Wang, C. Y. Shen and J. G. Jiang, *Pharmacol Res*, 2019, **150**, 104520.
19. M. Prasad, S. Jayaraman, S. R. Natarajan, V. P. Veeraraghavan, R. Krishnamoorthy, M. K. Gatasheh, C. P. Palanisamy and M. Elrobb, *Int J Biol Macromol*, 2023, **253**, 127242.
20. E. N. Cinar and N. Sanlier, *Plant Foods Hum Nutr*, 2025, **80**, 129.
21. S. Shityakov, E. Bigdelian, A. A. Hussein, M. B. Hussain, Y. C. Tripathi, M. U. Khan and M. A. Shariati, *Eur J Med Chem*, 2019, **176**, 149–161.
22. W. Cheng, S. Liu, J. He, H. Li, X. Liu, Z. Hu, X. Wang, Z. Wu, G. Xu, W. Liu and B. Liu, *Biochem Biophys Res Commun*, 2025, **749**, 151323.
23. M. Meghwal and T. K. Goswami, *Phytother Res*, 2013, **27**, 1121–1130.
24. W. Ternes and E. L. Krause, *Anal Bioanal Chem*, 2002, **374**, 155–160.
25. É. Szőke, É. Lemberkovics and L. Kursinszki, in *Natural Products*, eds. K. G. Ramawat and J. M. Mérillon, Springer-Verlag Berlin Heidelberg, Berlin, 2013, ch. 11, pp. 303–341.
26. A. Banerji and P. C. Ghosh, *Tetrahedron*, 1973, **29**, 977–979.
27. M. I. Addae and F. G. Torto, *Tetrahedron Lett.*, 1976, **17**, 3049–3050.
28. A. Bauer, J.-H. Nam and N. Maulide, *Synlett*, 2019, **30**, 413–416.
29. X. Tian, M. Zhou, J. Ning, X. Deng, L. Feng, H. Huang, D. Yao and X. Ma, *J Enzyme Inhib Med Chem*, 2021, **36**, 737–748.
30. R. A. Olsen and G. O. Spessard, *J. Agric. Food Chem.*, 1981, **29**, 942–944.
31. J. C. Sloop, *J. Chem. Educ.*, 1995, **72**, 25–27.
32. C. J. Teskey, P. Adler, C. R. Goncalves and N. Maulide, *Angew Chem Int Ed Engl*, 2019, **58**, 447–451.
33. M. S. Keerthana and M. Jeganmohan, *Chem Commun (Camb)*, 2022, **58**, 8814–8817.
34. G. F. Pan, X. L. Zhang, X. Q. Zhu, R. L. Guo and Y. Q. Wang, *iScience*, 2019, **20**, 229–236.
35. H. Li, M.-L. Wang, Y.-W. Liu, L.-J. Li, H. Xu and H.-X. Dai, *ACS Catalysis*, 2021, **12**, 82–88.
36. S. Tauboi and A. Takeda, *Tetrahedron Lett.*, 1979, **20**, 1043–1044.
37. J. G. Geisler and G. G. Gross, *Phytochemistry*, 1990, **29**, 489–492.
38. P. M. Dewick, *Medicinal natural products A biosynthetic approach*, Wiley, United Kingdom, 2009.
39. S. K. Okwute and H. O. Egharevba, *International Journal of Chemistry*, 2013, **5**.



40. A. Schnabel, F. Cotinguiba, B. Athmer, C. Yang, B. Westermann, A. Schaks, A. Porzel, W. Brandt, F. Schumacher and T. Vogt, *Plant J*, 2020, **102**, 569–581.
41. Z. Jin, J. Wungsintaweekul, S. H. Kim, J. H. Kim, Y. Shin, D. K. Ro and S. U. Kim, *Biochem J*, 2020, **477**, 61–74.
42. Y. Lv, J. Zhu, S. Huang, X. Xing, S. Zhou, H. Yao, Z. Yang, L. Liu, S. Huang, Y. Miao, X. Liu, A. R. Fernie, Y. Ding and J. Luo, *Plant J*, 2024, **117**, 107–120.
43. G. J. Gatto, N. L. Boyne, N. L. Kelleher and C. T. Walsh, *J. Am. Chem. Soc.*, 2006, **128**, 3838–3847.
44. D. Babadi, S. Dadashzadeh, Z. Shahsavari, S. Shahhosseini, T. L. M. Ten Hagen and A. Haeri, *Int J Pharm*, 2022, **624**, 121990.
45. S. Li, Y. Lei, Y. Jia, N. Li, M. Wink and Y. Ma, *Phytomedicine*, 2011, **19**, 83–87.
46. H. K. Matthews, C. Bertoli and R. A. M. de Bruin, *Nat Rev Mol Cell Biol*, 2022, **23**, 74–88.
47. A. L. Greenshields, C. D. Doucette, K. M. Sutton, L. Madera, H. Annan, P. B. Yaffe, A. F. Knickle, Z. Dong and D. W. Hoskin, *Cancer Lett*, 2015, **357**, 129–140.
48. E. J. Han, E. Y. Choi, S. J. Jeon, S. W. Lee, J. M. Moon, S. H. Jung and J. Y. Jung, *Int. J. Mol. Sci.*, 2023, **24**, 13949.
49. J. Xia, P. Guo, J. Yang, T. Zhang, K. Pan and H. Wei, *Biochem Biophys Res Commun*, 2024, **728**, 150340.
50. C. D. Doucette, A. L. Hilchie, R. Liwski and D. W. Hoskin, *J Nutr Biochem*, 2013, **24**, 231–239.
51. S. Li, T. T. Nguyun, T. T. Ung, D. K. Sah, S. Y. Park, V. K. Lakshmanan and Y. D. Jung, *Antioxidants*, 2022, **11**, 530.
52. A. Senrunga, T. Tripathi, J. Yadav, D. Janjua, A. Chaudhary, A. Chhokar, N. Aggarwal, U. Joshi, N. Goswami and A. C. Bharti, *BMC Cancer*, 2023, **23**, 1173.
53. C. R. Quijia and M. Chorilli, *Phytother Res*, 2022, **36**, 147–163.
54. A. Manayi, S. M. Nabavi, W. N. Setzer and S. Jafari, *Curr Med Chem*, 2018, **25**, 4918–4928.
55. W. W. Xu, Y. M. Xiao, L. Zheng, M. Y. Xu, X. H. Jiang and L. Wang, *Pharmaceutics*, 2023, **15**, 2703.
56. Z. Zuo, X. Liu, X. Qian, T. Zeng, L. Sang, H. Liu, Y. Zhou, L. Tao, X. Zhou, N. Su, Y. Yu, Q. Chen, Y. Luo and Y. Zhao, *J Med Chem*, 2020, **63**, 7633–7652.
57. C. Mao, X. Liu, Y. Zhang, G. Lei, Y. Yan, H. Lee, P. Koppula, S. Wu, L. Zhuang, B. Fang, M. V. Poyurovsky, K. Olszewski and B. Gan, *Nature*, 2021, **593**, 586–590.
58. J. F. Zhang, L. H. Hong, S. Y. Fan, L. Zhu, Z. P. Yu, C. Chen, L. Y. Kong and J. G. Luo, *Bioorg Chem*, 2024, **150**, 107594.
59. Z. Liu, Q. Hu, W. Wang, S. Lu, D. Wu, S. Ze, J. He, Y. Huang, W. Chen, Y. Xu, W. Lu and J. Huang, *Biochemical Pharmacology*, 2020, **177**.
60. P. Umadevi, K. Deepti and D. V. R. Venugopal, *Medicinal Chemistry Research*, 2013, **22**, 5466–5471.
61. V. Rama Subba Rao, G. Suresh, R. Ranga Rao, K. Suresh Babu, G. Chashoo, A. K. Saxena and J. Madhusudana Rao, *Medicinal Chemistry Research*, 2010, **21**, 38–46.
62. S. Shankar, M. M. Faheem, D. Nayak, N. A. Wani, S. Farooq, S. Koul, A. Goswami and R. Rai, *Bioconjug Chem*, 2018, **29**, 164–175.
63. L. F. Fan, X. M. Cao, H. J. Yan, Q. Wang, X. X. Tian, L. Zhang, X. Y. He, G. Borjihan and Morigen, *Oncotarget*, 2017, **8**, 47250–47268.
64. X. Tian, J. Lu, K. Nanding, L. Zhang, Y. Liu, M. Mailisu, M. Morigen and L. Fan, *Front Oncol*, 2022, **12**, 828160.
65. X.-J. Wang, H.-J. Chen, Z.-Y. Liu, Y. Qiao, X.-B. Wang, B.-Y. Wang, W.-T. Jiang, X. Hou, M.-M. Wang, K.-Q. Li, S.-Y. Zhang, H.-X. Li, B. Liu, J. Ji and M.-L. Yang, *Russian Journal of Organic Chemistry*, 2024, **60**, 1288–1300.
66. L. Zhang, S. Liu, D. Wang, X. Zhang, Z. Hu, X. Zou, X. Li, X. Wang, D. Xu, W. Liu and B. Liu, *Sci Rep*, 2025, **15**, 33541.
67. K. R. Amperayani and U. D. Parimi, *Russian Journal of General Chemistry*, 2019, **89**, 2301–2307.
68. S. B. Syed, H. Arya, I. H. Fu, T. K. Yeh, L. Periyasamy, H. P. Hsieh and M. S. Coumar, *Sci Rep*, 2017, **7**, 7972.
69. S. B. Syed, S. Y. Lin, H. Arya, I. H. Fu, T. K. Yeh, M. R. C. Charles, L. Periyasamy, H. P. Hsieh and M. S. Coumar, *Chem Biol Drug Des*, 2021, **97**, 51–66.
70. M. Zhong, L. Chen, Y. Tao, J. Zhao, B. Chang, F. Zhang, J. Tu, W. Cai and B. Zhang, *Bioorg Chem*, 2023, **138**, 106589.
71. L. Somsakeesit, A. Joompang, S. Phosri, P. Srikoorn, P. Kumboonma, T. Senawong and C. Phasosiri, *Songklanakarinn J. Sci. Technol.*, 2022, **44**, 1481–1488.
72. S. Phosri, A. Naladta, N. Teerakulkittipong, L. O. Somsakeesit, S. Tastub, N. Nualkaew and A. Joompang, *Biochem Biophys Res Commun*, 2025, **766**, 151895.
73. X. J. Wang, Y. Qiao, X. S. Wang, S. Y. Zhang, H. X. Li, H. H. Hao, K. Q. Li, S. J. Ma, Q. J. Zhu, J. Ji and B. Liu, *Fitoterapia*, 2024, **177**, 106118.
74. D. M. Elimam, A. A. Elgazar, A. Bonardi, M. Abdelfadil, A. Nocentini, R. A. El-Domany, H. A. Abdel-Aziz, F. A. Badria, C. T. Supuran and W. M. Eldehna, *Eur J Med Chem*, 2021, **225**, 113800.
75. D. M. Elimam, A. A. Elgazar, F. F. El-Senduny, R. A. El-Domany, F. A. Badria and W. M. Eldehna, *J Enzyme Inhib Med Chem*, 2022, **37**, 39–50.
76. A. H. Tantawy, X. G. Meng, A. A. Marzouk, A. Fouad, A. H. Abdelazeem, B. G. M. Youssif, H. Jiang and M. Q. Wang, *Rsc Adv*, 2021, **11**, 25738–25751.
77. S. K. Xu, Z. M. Jia, W. Q. Liu, Y. Z. Gu, J. H. Xi, J. Xu, G. Z. Yang, X. Z. Yang and Y. Chen, *Nat Prod Res*, 2024, 1–6.
78. L. H. Al-Wahaibi, M. A. Mahmoud, Y. A. Mostafa, A. E. Raslan and B. G. M. Youssif, *J Enzyme Inhib Med Chem*, 2023, **38**, 376–386.
79. C. Zhou, J. Wang, L. Zhou, H. Li, X. Liu, S. Wang, X. Zhang, X. Ye, H. Ren, K. Zeng, X. Li, D. Wang and J. Ji, *Bioorg Med Chem Lett*, 2025, **123**, 130231.
80. X. J. Wang, W. N. Jiang, J. J. He, H. J. Chen, Y. Qiao, D. Wang, B. Y. Wang, X. Hou, W. Liu, T. Geng, S. Y. Zhang, X. Liu, S. J. Ma, B. Liu, M. L. Yang and J. Ji, *Chem. J. Chin. Univ. -Chin.*, 2024, **45**.
81. M. Zhang, R. Liu, W. Jiang, H. Li, S. Zhang, W. Cheng, X. Ye, J. He, Y. Liu, A. Jing, Y. Song, D. Wang, X. Liu, B. Zhang, X. Wang and J. Ji, *Naunyn Schmiedebergs Arch Pharmacol*, 2025, **398**, 7121–7131.
82. X. J. Wang, B. Y. Wang, B. Zhang, L. Chen, K. Q. Li, M. M. Wang, H. H. Hao, M. X. Lu, X. X. Shen, Y. K. Sun, Z. D. Gao, Z. Y. Yan, Z. Y. Lang, M. J. Yu, Z. J. He, S. J. Ma, J. Ji and Y. L. Chang, *Fitoterapia*, 2025, **187**, 106911.
83. J. Santos, M. Brito, R. Ferreira, A. P. Moura, T. Sousa, T. Batista, V. Manguera, F. Leite, R. Cruz, G. Vieira, B. Lira, P. Athayde-Filho, H. Souza, N. Costa, R. Veras, J. M. Barbosa-Filho, H. Magalhaes and M. Sobral, *Int J Mol Sci*, 2018, **19**.
84. R. C. Ferreira, T. M. Batista, S. S. Duarte, D. K. F. Silva, T. M. H. Lisboa, R. F. P. Cavalcanti, F. C. Leite, V. M. Manguera, T. K. G. Sousa, R. A. Abrantes, E. O. D. Trindade, P. F. Athayde-Filho, M. C. R. Brandao, K. C. P. Medeiros, D. F.



ARTICLE

Journal Name

- Farias and M. V. Sobral, *Biomed Pharmacother*, 2020, **128**, 110247.
85. P. Zhu, J. Qian, Z. Xu, C. Meng, J. Liu, W. Shan, W. Zhu, Y. Wang, Y. Yang, W. Zhang, Y. Zhang and Y. Ling, *J Nat Prod*, 2020, **83**, 3041–3049.
86. K. Zhang, X. Yang, Y. Wang, Y. Yu, N. Huang, G. Li, X. Li, J. C. Wu and S. Yang, *Nat Med*, 2025, **31**, 45–59.
87. L. Huang, X. H. Huang, X. Yang, J. Q. Hu, Y. Z. Zhu, P. Y. Yan and Y. Xie, *Pharmacol Res*, 2024, **201**, 107100.
88. K. H. Wong, Y. Wang, X. Wang, Y. Yin, K. Feng and M. Chen, *J Control Release*, 2025, **382**, 113656.
89. H. Heidari, M. Bagherniya, M. Majeed, T. Sathyapalan, T. Jamialahmadi and A. Sahebkar, *Phytother Res*, 2023, **37**, 1462–1487.

View Article Online
DOI: 10.1039/D6MD00223D



Data sharing does not apply to this article as no datasets were generated or analysed during the current study.

[View Article Online](#)

DOI: 10.1039/D6MD00223D

